A fluorescent chemosensor for wide-range pH detection†

Go Nishimura, Yasuhiro Shiraishi* and Takayuki Hirai

Received (in Cambridge, UK) 9th June 2005, Accepted 5th September 2005
First published as an Advance Article on the web 23rd September 2005
DOI: 10.1039/b508136j

Simple polyamines, L1–L3, bearing anthracene and benzophenone units at the respective ends, behave as a fluorescent pH sensor applicable to wide-range pH detection.

Design of supramolecular systems enabling a fluorimetric detection of chemical species in solution has attracted much attention.[1] Much effort has been made toward development of a fluorescent pH sensor (H^+ detection).[2] The simplest pH sensing system consists of a fluorophore (*e.g.*, anthracene) covalently linked to a polyamine.[3] In this system, the fluorescence intensity (I_F) of the fluorophore decreases with an increase in pH of the solution. This occurs because deprotonation of the nitrogen atom, associated with a pH increase, leads to an electron transfer (ELT) from the nitrogen atom to a photoexcited fluorophore.[4] The ELT process depends strongly on the distance from the nitrogen atom to the fluorophore,[5] such that the deprotonation of the "crucial" nitrogen atom triggers a drastic I_F decrease. The pH–I_F profile, therefore, usually demonstrates a single or double sigmoidal curve with pK_a' 1–8.[6] Most of the pH sensors therefore detect only in a limited pH range.

Here we report a family of polyamines bearing anthracene (AN) and benzophenone (BP) moieties at the respective ends, **L1**–**L3** (Scheme 1), as a new fluorescent pH sensor applicable to a wide-range pH detection: the pH–I_F plots of these molecules demonstrate a "gentle slope" profile over the pH 2–10 range. This function involves pH-controlled two consecutive intramolecular ELT processes: (i) ELT from photoexcited AN to BP [ELT(AN* → BP)]; and (ii) ELT from the nitrogen atom to the photoexcited AN [ELT(N → AN*)].

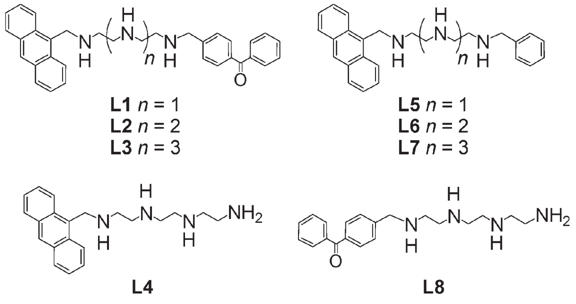

Scheme 1 Structure of polyamines, **L1**–**L8**.

L1–**L3** show distinctive fluorescence at 380–540 nm in water, attributable to an emission from photoexcited AN (Fig. S1 and S4†). Fig. 1A shows fluorescence spectra of **L2** (λ_{ex} = 368 nm) for instance. Polyamine bearing a single AN unit at one end (**L4**) and polyamines bearing AN and benzene units at the respective ends (**L5**–**L7**) show similar spectra (Fig. S5–S8†). The I_F of **L4**–**L7** at 416 nm, when plotted against pH, demonstrates a single sigmoidal curve with pK_a' 6.2–7.8 (Fig. S5–S8†); as shown in Fig. 1B (open symbol), **L6** shows the typical example with pK_a' 6.7. In **L4**–**L7** systems, the I_F at pH 1–5 is almost constant (Fig. S5–S8†), indicating that these can only detect pH 5–10. However, for **L1**–**L3** (Fig. S1 and S4†), the pH–I_F profile is a "gentle slope" over pH 2–10 range (Fig. 1B, closed symbol; for example **L2**), suggesting that **L1**–**L3** allows a wide-pH range detection.

Dotted lines in Fig. 1B denote mole fraction distribution of the different protonated species of **L2**, calculated from the protonation constants, which were determined potentiometrically.[7] **L6** shows almost the same distribution as that of **L2** (Fig. S7†). The deprotonation sequence of **L6** determined by ^1H and ^{13}C NMR reveals that: (i) first deprotonation occurs on the third nitrogen

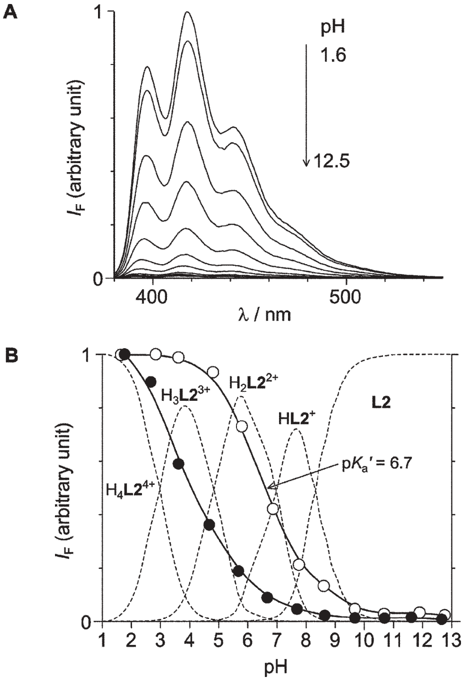

Fig. 1 (A) Change in fluorescence spectra (λ_{ex} = 368 nm) of **L2** (40 μM) in aqueous NaCl (0.15 M) solution with pH. (B) Change in fluorescence intensity of **L2** (●) and **L6** (○) at 416 nm with pH and mole fraction distribution of the protonation states of **L2** (dotted line). The fluorescence quantum yield (Φ_f) at pH 1.6 is 0.23 (**L2**) and 0.38 (**L6**).

Research Center for Solar Energy Chemistry, and Division of Chemical Engineering, Graduate School of Engineering Science, Osaka University, Toyonaka, 560-8531, Japan. E-mail: shiraish@cheng.es.osaka-u.ac.jp; Fax: +81 6 6850 6273; Tel: +81 6 6850 6271

† Electronic supplementary information (ESI) available: Properties and spectra of **L1**–**L8** compounds (including: Fig. S1–S11, Scheme S1, Tables S1–S10). See http://dx.doi.org/10.1039/b508136j

atom from the AN unit; (ii) the second deprotonation occurring on the second nitrogen atom from the AN unit leads to a partial emission quenching (*ca.* 30%); and (iii) total emission quenching occurs upon removal of the third proton from the first nitrogen atom from AN. These indicate that the ELT(N → AN*) process within **L6** is triggered by the second deprotonation. The deprotonation sequence of **L2** is the same as that of **L6**, suggesting that **L2** involves other emission quenching processes at pH 2–5, where $H_3\mathbf{L2}^{3+}$ species exist predominantly.

The molar extinction coefficient of **L4** bearing a single AN end, measured at 368 nm (pH 2.6), is 16-fold higher than that of **L8** bearing a single BP end (Fig. S9†). This indicates that, for **L2** bearing AN and BP ends, excitation light (λ_{ex} = 368 nm) is mostly absorbed by the AN moiety, and hence, excitation of the BP moiety is suppressed. Singlet excitation energy of AN (E_{0-0}^{AN}) and reduction potential of AN [$E(AN/AN^-)$] are 3.28 eV and −1.92 V (*vs.* SCE in MeCN), respectively,[8] and oxidation potential of BP [$E(BP^+/BP)$] is +2.65 V.[9] Hence, free energy change in ELT from BP to excited AN, $\Delta G_{ELT(BP \rightarrow AN^*)}$ (= $-[E_{0\text{-}0}^{AN} + eE(AN/AN^-) - eE(BP^+/BP)]$),[8] shows positive value (+1.29 eV), indicating that the process is not favored thermodynamically. In contrast, the free energy change in ELT from excited AN to BP,[10] $\Delta G_{ELT(AN^* \rightarrow BP)}$, shows a negative value (−0.36 eV),[11] indicating that the process is allowed thermodynamically. E_{0-0}^{AN} is higher than E_{0-0}^{BP} (3.22 eV)[9] and hence also allows energy transfer (ENT) from singlet excited-state AN to BP. However, the free energy change in the process (−0.05 eV) is much lower than that of ELT(AN* → BP) (−0.36 eV). These findings strongly indicate that the ELT(AN* → BP) is involved in the **L2** fluorescence quenching at pH 2–5 (Fig. 1B, closed symbol). In the case of **L6**, free energy changes in both ELT(benzene → AN*) and ELT(AN* → benzene) processes show a positive value (+0.94 and +1.34 eV).[12] $E_{0-0}^{benzene}$ (4.76 eV)[8] is higher than E_{0-0}^{AN}, such that ENT(AN* → benzene) does not occur, resulting in the constant I_F at pH 2–5 (Fig. 1B, open symbol). When a mixture of **L4** and **L8** was used for fluorescence measurement, the obtained pH–I_F profile is almost the same as that obtained using only **L4** (Fig. S5†). This indicates that "intermolecular" ELT(AN* → BP) does not occur; "intramolecular" ELT(AN* → BP) within **L1**–**L3** is then the crucial factor triggering the "gentle slope" response.

As shown in Fig. 1B, at strongly acidic pH (<3) where $H_4\mathbf{L2}^{4+}$ species exist predominantly, contribution of the ELT(AN* → BP) process to the I_F of **L2** is minor. This may be ascribed to a large electrostatic repulsion of the protonated amines, as reported for the related polyamines,[13] which suppresses the required bending movement of the polyamine chain for the ELT. UV-vis measurement revealed a pH-induced red-shift of the absorption spectra of **L2** (Fig. S2†) attributable to a dipole–dipole interaction between AN and BP,[14] while no change was observed for **L6** (Fig. S7†). ^1H NMR titration of **L2** in D_2O/CD_3CN (80/20 *v*/*v*) revealed a corresponding upper-field shift of AN and BP resonances with a pH increase (Fig. S3†).[15] These suggest that the pH increase actually brings these moieties closer.

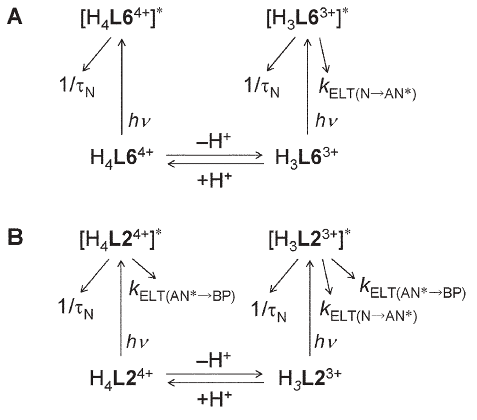

Scheme 2 Decay kinetics for (A) **L6** and (B) **L2** species ($1/\tau_N$: rate constant due to natural decay, $k_{ELT(N \rightarrow AN^*)}$: rate constant due to ELT(N → AN*), $k_{ELT(AN^* \rightarrow BP)}$: rate constant due to ELT(AN* → BP)).

To clarify the mechanism of the "gentle slope" response of **L1**–**L3**, time-resolved fluorescence measurement was employed. Broad analysis over pH 1–12 indicates that fluorescence decays of **L1**–**L7** are explained with the sums of two or three exponentials (Fig. S10 and Tables S2–S7†). The decay kinetics of **L6** and **L2** can be interpreted as shown in Scheme 2. In both cases, ground-state equilibrium exists between species of higher ($H_n\mathbf{L}^{n+}$) and lower ($H_{n-1}\mathbf{L}^{(n-1)+}$) protonation degree. Simultaneous excitation of both species leads to a formation of excited $H_n\mathbf{L}^{n+*}$ and $H_{n-1}\mathbf{L}^{(n-1)+*}$ species. In the case of **L6**, the fully protonated $H_4\mathbf{L6}^{4+*}$ decays with a rate constant equal to the reciprocal of τ_N, while $H_3\mathbf{L6}^{3+*}$ involves an additional quenching process due to ELT(N → AN*) with a rate constant, $k_{ELT(N \rightarrow AN^*)}$; the overall decay rate constant of $H_n\mathbf{L6}^{n+*}$, $k_{\mathbf{L6}}$, is expressed as $1/\tau_N + k_{ELT(N \rightarrow AN^*)}$ (Scheme 2A).[4a,13b] In the **L2** system, the rate constant due to ELT(AN* → BP), $k_{ELT(AN^* \rightarrow BP)}$, must be considered (Scheme 2B). Hence, the overall decay rate constant of $H_n\mathbf{L2}^{n+*}$, $k_{\mathbf{L2}}$, is expressed as $1/\tau_N + k_{ELT(N \rightarrow AN^*)} + k_{ELT(AN^* \rightarrow BP)}$.

The $1/\tau_N$ value for all of the $H_n\mathbf{L6}^{n+*}$ and $H_n\mathbf{L2}^{n+*}$ species is constant, and the $k_{ELT(N \rightarrow AN^*)}$ value for respective $H_n\mathbf{L6}^{n+*}$ and $H_n\mathbf{L2}^{n+*}$ species, of the same protonation degree, should be equal. Hence, the $k_{ELT(AN^* \rightarrow BP)}$ value for respective $H_n\mathbf{L2}^{n+*}$ species is obtained by subtracting the overall decay rate constant of $H_n\mathbf{L6}^{n+*}$ from that of $H_n\mathbf{L2}^{n+*}$, $k_{\mathbf{L2}}$–$k_{\mathbf{L6}}$.[16] As summarized in Table 1, the contribution of the ELT(AN* → BP) quenching to the overall decay ($k_{ELT(AN^* \rightarrow BP)}/k_{\mathbf{L2}}$) for $H_3\mathbf{L2}^{3+*}$ (75%) is much higher than that for $H_4\mathbf{L2}^{4+*}$ (33%) and that for species of lower protonation degree (<6%). This suggests that the first deprotonation of **L2** triggers ELT(AN* → BP) (Scheme 3). The contribution of ELT(N → AN*) quenching is increased to 0% ($H_3\mathbf{L2}^{3+*}$), 15% ($H_2\mathbf{L2}^{2+*}$), 66% ($H\mathbf{L2}^{+*}$), and 84% (**L2***), indicating that the second deprotonation ($H_2\mathbf{L2}^{2+}$ formation) triggers ELT(N → AN*), and further deprotonations lead to complete fluorescence quenching. These indicate that the ELT(AN* → BP) and ELT(N → AN*) processes, occurring sequentially with **L2** deprotonation (Scheme 3), leads to the "gentle slope" response.

Another interesting aspect of the **L1**–**L3** molecules bearing AN and BP moieties is that the slope of the pH–fluorescence intensity profile changes depending on the chain length of the polyamine (see graphical abstract): the slope tends to be "gentler" with longer chain length: **L3** > **L2** ⩾ **L1**. The fluorescence quenching behavior of **L1** and **L3** is analogous to that of **L2**: the first deprotonation triggers ELT(AN* → BP) and the second (and later) deprotonation triggers ELT(N → AN*) (Fig. S11 and Tables S8 and S9†). The gentler slope of **L3** is explained as follows: on the mono-deprotonated **L3** species, ELT(AN* → BP) occurs more slowly ($2.15 \times 10^8\ s^{-1}$) than on the corresponding **L2** species (Table S9†),

Table 1 Fluorescence quenching rate constants for respective **L2** species of different protonation degree[a]

	$H_4\mathbf{L2}^{4+}$	$H_3\mathbf{L2}^{3+}$	$H_2\mathbf{L2}^{2+}$	$H\mathbf{L2}^{+}$	**L2**
$k_{\mathbf{L2}}/10^8\ s^{-1}$	1.28	3.47	1.09	2.69	5.68
$k_{ELT(N \rightarrow AN^*)}/10^8\ s^{-1}$ [contribution (%)][b]	0 (0)	0.01 (0)	0.17 (15)	1.77 (66)	4.79 (84)
$k_{ELT(AN^* \rightarrow BP)}/10^8\ s^{-1}$ [contribution (%)[c]]	0.43 (33)	2.60 (75)	0.07 (6)	0.06 (2)	0.03 (1)

[a] $1/\tau_N$: 8.55×10^7 (s^{-1}). [b] $k_{ELT(N \rightarrow AN^*)}/k_{\mathbf{L2}} \times 100$. [c] $k_{ELT(AN^* \rightarrow BP)}/k_{\mathbf{L2}} \times 100$.

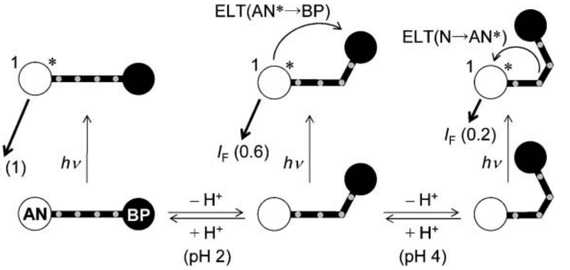

Scheme 3 Schematic representation for the mechanism of "gentle slope" fluorescence response of **L2**.

because of a longer distance between the AN and BP moieties due to a low angular bending of the long polyamine chain.[13] ELT(N → AN*) also occurs more slowly on the **L3** species of lower protonation degree, because of delocalization of positive charges along the polyamine chain.[14] On respective **L1** species, ELT(AN* → BP) and ELT(N → AN*) occur more rapidly (Fig. S11 and Table S8†), but the slope of **L1** is nearly the same as that of **L2**. This is because deprotonation of **L1** occurs at higher pH than that of **L2** (*i.e.* **L1** has higher protonation constants than **L2**) because of a smaller number of nitrogens.

In summary, we have demonstrated that the simple-structured polyamines, **L1**–**L3**, bearing AN and BP moieties at respective ends, behave as a fluorescent pH sensor applicable to a wide-range pH detection. The concept for molecular design presented here, based on sequential electron transfer, may contribute to the development of a more convenient fluorescent chemosensor.

This work was supported by the Grant-in-Aid for Scientific Research (No. 15360430) and on Priority Areas (417) (No. 17029037) from the Ministry of Education, Culture, Sports, Science and Technology, Japan (MEXT). G. N. acknowledges the Research Fellowship of the Japan Society for the Promotion of Science (JSPS) for Young Scientists.

Notes and references

1 (*a*) *Fluorescent Chemosensors for Ion and Molecular Recognition*, ed. A. W. Czarnik, American Chemical Society, Washington DC, 1993; (*b*) A. P. de Silva, H. Q. N. Gunaratne, T. Gunnlaugsson, A. J. M. Huxley, C. P. McCoy, J. T. Rademacher and T. E. Rice, *Chem. Rev.*, 1997, **97**, 1515; (*c*) B. Valeur and I. Leray, *Coord. Chem. Rev.*, 2000, **205**, 3; (*d*) L. Fabbrizzi, M. Licchelli and A. Taglietti, *Dalton Trans.*, 2003, 3471; (*e*) R. Martínez-Máñez and F. Sancenón, *Chem. Rev.*, 2003, **103**, 4419.

2 (*a*) S. G. Schulman, S. Chen, F. Bai, M. J. P. Leiner, L. Weis and O. S. Wolfbeis, *Anal. Chim. Acta*, 1995, **304**, 165; (*b*) G. Liebsch, I. Klimant, C. Krause and O. S. Wolfbeis, *Anal. Chem.*, 2001, **73**, 4354; (*c*) H. R. Kermis, Y. Kostov, P. Harms and G. Rao, *Biotechnol. Prog.*, 2002, **18**, 1047; (*d*) K. M.-C. Wong, W.-S. Tang, X.-X. Lu, N. Zhu and V. W.-W. Yam, *Inorg. Chem.*, 2005, **44**, 1492; (*e*) T. Gunnlaugsson, C. P. McCoy and F. Stomeo, *Tetrahedron Lett.*, 2004, **45**, 8403; (*f*) S. Charier, O. Ruel, J.-B. Baudin, D. Alcor, J.-F. Allemand, A. Meglio and L. Jullien, *Angew. Chem., Int. Ed.*, 2004, **43**, 4785.

3 (*a*) E. U. Akkaya, M. E. Huston and A. W. Czarnik, *J. Am. Chem. Soc.*, 1990, **112**, 3590; (*b*) S. Alves, F. Pina, M. T. Albelda, E. García-España, C. Soriano and S. V. Luis, *Eur. J. Inorg. Chem.*, 2001, 405.

4 (*a*) G. Greiner and I. Maier, *J. Chem. Soc., Perkin Trans. 2*, 2002, 1005; (*b*) L. M. Daffy, A. P. de Silva, H. Q. N. Gunaratne, C. Huber, P. L. M. Lynch, T. Werner and O. S. Wolfbeis, *Chem. Eur. J.*, 1998, **4**, 1810.

5 (*a*) F. Pina, J. C. Lima, C. Lodeiro, J. Seixas de Melo, P. Díaz, M. T. Albelda and E. García-España, *J. Phys. Chem. A*, 2002, **106**, 8207; (*b*) L. Rodríguez, S. Alves, J. C. Lima, A. J. Parola, F. Pina, C. Soriano, T. Albelda and E. García-España, *J. Photochem. Photobiol. A*, 2003, **159**, 253; (*c*) F. Pina, M. J. Melo, M. A. Bernardo, S. V. Luis and E. García-España, *J. Photochem. Photobiol. A*, 1999, **126**, 65.

6 For example: (*a*) X. Guo, X. Qian and L. Jia, *J. Am. Chem. Soc.*, 2004, **126**, 2272; (*b*) T. Gunnlaugsson, T. C. Lee and R. Parkesh, *Tetrahedron*, 2004, **60**, 11239; (*c*) F. Pina, M. A. Bernardo and E. García-España, *Eur. J. Inorg. Chem.*, 2000, 2143; (*d*) L. Prodi, F. Bolletta, M. Montalti, N. Zaccheroni, P. B. Savage, J. S. Bradshaw and R. M. Izatt, *Tetrahedron Lett.*, 1998, **39**, 5451.

7 Potentiometric measurements were carried out in aqueous NaCl (0.15 M) solution at 298 K. The program HYPERQUAD (A. Sabatini, A. Vacca and P. Gans, *Coord. Chem. Rev.*, 1992, **120**, 389) was employed for the determination of the protonation constants. The stepwise protonation constants for **L2** are: $\log K(H\mathbf{L2}/H\cdot\mathbf{L2}) = 8.53$, $\log K(H_2\mathbf{L2}/H\mathbf{L2}\cdot H) = 7.12$, $\log K(H_3\mathbf{L2}/H_2\mathbf{L2}\cdot H) = 5.01$, $\log K(H_4\mathbf{L2}/H_3\mathbf{L2}\cdot H) = 3.12$. The constants for the other materials: see Table S1†.

8 (*a*) T. D. S. Cruz, D. L. Akins and R. L. Birke, *J. Am. Chem. Soc.*, 1976, **98**, 1677; (*b*) L. Fabbrizzi, M. Licchelli, P. Pallavicini and A. Taglietti, *Inorg. Chem.*, 1996, **35**, 1733.

9 (*a*) *Handbook of Photochemistry*, ed. S. L. Murov, I. Carmichael and G. L. Hug, Marcel Dekker, New York, 1993; (*b*) P. Jacques, X. Allonas, A. Sarbach, E. Haselbach and E. Vauthey, *Chem. Phys. Lett.*, 2003, **378**, 185.

10 (*a*) B.-W. Zhang, Y. Cao, J.-W. Bai and J.-R. Chen, *J. Photochem. Photobiol. A*, 1997, **106**, 169; (*b*) T. Hirsch, H. Port, H. C. Wolf, B. Miehlich and F. Effenberger, *J. Phys. Chem. B*, 1997, **101**, 4525.

11 $\Delta G_{ELT(AN^* \rightarrow BP)} = -[E_{0\text{-}0}{}^{AN} + eE(BP/BP^-) - eE(AN^+/AN)]$, where $E(BP/BP^-) = -1.72$ V *vs.* SCE in MeCN; $E(AN^+/AN) = 1.20$ V *vs.* SCE in MeCN (ref. 8 and 9).

12 $E(\text{benzene}/\text{benzene}^-) = -3.42$ V *vs.* SCE in dimethoxyethane and $E(\text{benzene}^+/\text{benzene}) = 2.30$ V *vs.* SCE in MeCN; M. John and H. Juergen, *Angew. Chem.*, 1984, **96**, 64.

13 (*a*) Y. Shirashi, Y. Tokitoh, G. Nishimura and T. Hirai, *Org. Lett.*, 2005, **7**, 2611; (*b*) M. T. Albelda, M. A. Bernardo, P. Díaz, E. García-España, J. Seixas de Melo, F. Pina, C. Soriano and S. V. Luis, *Chem. Commun.*, 2001, 1520.

14 (*a*) A. A. Lamola, P. A. Leermakers, G. W. Byers and G. S. Hammond, *J. Am. Chem. Soc.*, 1965, **87**, 2322; (*b*) I. Tinoco, Jr., *J. Am. Chem. Soc.*, 1960, **82**, 4785.

15 (*a*) V. Steullet and D. W. Dixon, *J. Chem. Soc., Perkin Trans. 2*, 1999, 1547; (*b*) T. Itahara, *J. Chem. Soc., Perkin Trans. 2*, 1998, 1455.

16 M. T. Albelda, P. Díaz, E. García-España, J. C. Lima, C. Lodeiro, J. Seixas de Melo, A. J. Parola, F. Pina and C. Soriano, *Chem. Phys. Lett.*, 2002, **353**, 63.